20-Mar-2020

Re: comments of the editors and Reviewers 2

Dear Dr. Richard Gloaguen:

We would like to express our sincere gratitude to the editors and anonymous reviews for their time and effort in handling our manuscript **(npg-2020-8)** entitled **"An enhanced correlation identification algorithm and its application on spread spectrum induced polarization data".**
We would like to say thanks again sincerely to the editors and anonymous reviews for their time and effort spent in handing our paper, as well as providing us many constructive comments for improving very much the presentation and quality of this manuscript.
It is worth pointing out that the reviewers' comments and suggestions have really constructively helped us improve further the quality and presentation of the manuscript. In light of their inspiring comments and suggestions, we have revised the manuscript duly and carefully, and the specific responses to the reviewers are listed as below, with the corresponding revisions **highlighted in blue color** in the revised manuscript.

Sincerely,
Dr. Siming He
hsmfly1982@163.com

Responses to comments of Reviewer 2

We greatly appreciate your suggestions, and we hope our revisions have addressed your questions and made this manuscript better.

Comment 1. The reference list needs to be updated. It should be alphabetic and the year should be at the end. See https://www.nonlinear-processes-in-geophysics.net/submission.html#manuscript composition for guide lines.

Response.

We have fixed this problem, checked and modified the literature formatting carefully according to the formatting guide.

Comment 2. Høyer et al. 2018 is missing from the reference list.

Response.

We have added it to the reference list.

Page 12, Line 33 to 35

The related reference is as follows:

Høyer, A. S., Klint, K. E. S., Fiandaca, G., Maurya, P. K., Christiansen, A. V., Balbarini, N., Bjerg, P. L., Hansen, T. B., and Møller, I.: Development of a high-resolution 3D geological model for landfill leachate risk assessment. Engineering Geology, 249, 45–59, https://doi:10.1016/j.enggeo.2018.12.015, 2015.

Comment 3. Page 1: "SSIP technology has a certain degree of noise immunity".

Response.

Sorry, what we are trying to say is that one of the advantages of this sequence is to be essentially spectrally flat in a given frequency range, which can be used in noise reduction technology (Liu et al., 2017).

We have replaced "SSIP technology has a certain degree of noise immunity" to "In field detection experiments, it is still a major problem that IP data is often contaminated with background noise."

Page 1, Line 34

The related reference is as follows:

Liu, W. Q., Chen, R. J., Cai, H. Z., Luo, W. B., and Revil, André.: Correlation analysis for spread spectrum induced polarization signal processing in electromagnetically noisy environments, Geophysics, 82, E243–E256, https://doi.org/10.1190/geo2016-0109.1, 2017.

Comment 4. Page 9, Line 1: Reference missing for Res2DInv.

Response.

We have added its to the reference list.

Page 10, Line 3 and 4

Page 12, Line 8 to 10

The related reference is as follows:

Arifin, M. H., Kayode, J. S., Izwan, M. K., Zaid, H. A. H., and Hussin, H.: Data for the potential gold mineralization mapping with the applications of Electrical Resistivity Imaging and Induced Polarization geophysical surveys, Data in Brief, 22, 830–835. doi:10.1016/j.dib.2018.12.086, 2019.

Comment 5. Page 9, Line 8, “red point”. I guess you are referring to Figure 8? Maybe just “data points”?

Response.

Thank you for pointing out our negligence. Data points are numbered according to Figure 11, and the related data points are modified.

Page 10 Line 1, 2 and 10

Page 11 Line 2

These modifications are as follows:

(1) To verify the reason of the improved detecting precision, the SDs of data points are calculated from 18 to 50 (Figure 10), as shown in Figure 11.

(2) Figure 13. Standard deviation (SD) of the ECI algorithm and the others to the data dots from No. 18 to 50 at 80Hz.

Comment 6. Page 9, Line 17, “algorithm” should be “algorithms”

Response.

We have replaced “algorithm” with “algorithms”.

Page 11, Line 4

Comment 7. Figure 8: What is the difference between blue and red dots? If there is no difference, I suggest that you use the same color.

Response.

Many thanks for your suggestion. We have changed all the red dots to blue dots.

Page 10, Line 1 and 2

This modifications is as follows:

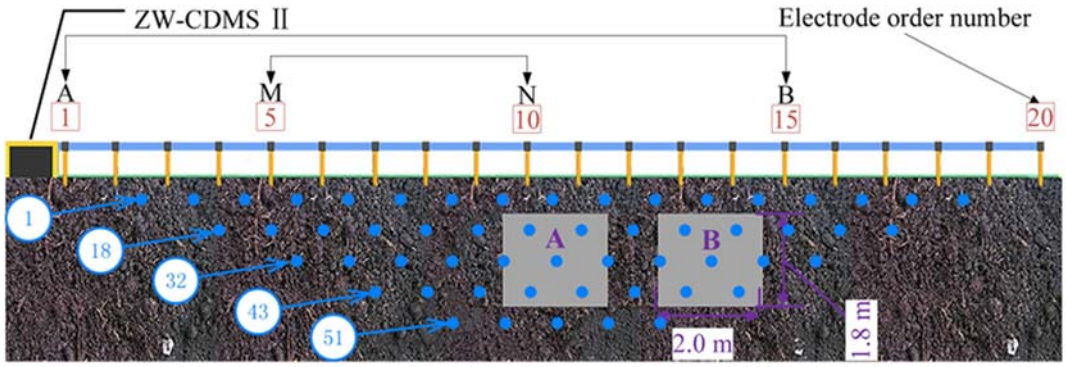

Figure 11. The schematic of the two high resistance cavities.

Comment 8. Figure 11: Please elaborate the figure text. What are the number in the plot?

Response.

We add more specific explanations for Figure 14 in Page 11, Line 5 to 7. This modification is as follows:

“For example, Figure 1(a) and (d) shows that the amplitude and phase of complex resistivity spectrum for this point at 80 Hz processed by FDIP are 39.7 Ω•m and -0.0881 rad, the amplitude and phase are 40.9 Ω•m and 6.12 rad when at 160Hz, and the amplitude and phase are 38.7 Ω•m and -0.253 rad when at 320Hz.”

Comment 9. Experiment:

a. What is the resistivity of the two cavities. It is difficult to access the inversion results, when the resistivity is unknown.

Response.

We employ the high-density resistivity method. This method is used to infer geological structure by utilizing the differences in the electrical conductivity between the loess and the two cavities. In the case of the known geological structure， we can verify the correctness of the inversion result according to the differences, as others have reported in the literature (Liu et al., 2017).

The related reference is as follows:

Liu, W. Q., Chen, R. J., Cai, H. Z., Luo, W. B., and Revil, André.: Correlation analysis for spread spectrum induced polarization signal processing in electromagnetically noisy environments, Geophysics, 82, E243–E256, https://doi.org/10.1190/geo2016-0109.1, 2017.

b. As commented by previous review, you need to show some data and data fits. So, a figure with the recorded data (resistivity and phase) and the forward response (resistivity and phase) of the final inversion model. This could be added to Figure 11.

Response.

We agree with your suggestion. Unfortunately, we did not have the forward response (resistivity and phase) about the model. As said in comment 9.a, the model is the known geological structure. The loess and the two cavities have the obvious conductive differences. Therefore, we can use the differences to infer the geological structure of the model. To verify the efficacy of the test system, we take a variety of measures.

(1) The loess is measured to have an electronic resistivity of 36 Ω•m 。

(2) Diagram of the field-test is added to the paper.

(3) We replace the simulation experiment with the resistance-capacitance experiment, present the recorded data and the forward response， and analyze the noise reduction performance on the frequency-spectrum by the three algorithms.

Page 9, Line 9, and 10

Page 9, Line 12 and 13

Page 6, Line 8 and 9

This modifications is as follows:

(1) The two cavities are buried by loess. The loess is measured to have an electronic resistivity of 36 Ω•m .

(2)

Figure 10. Diagram of the field-test.

(3)

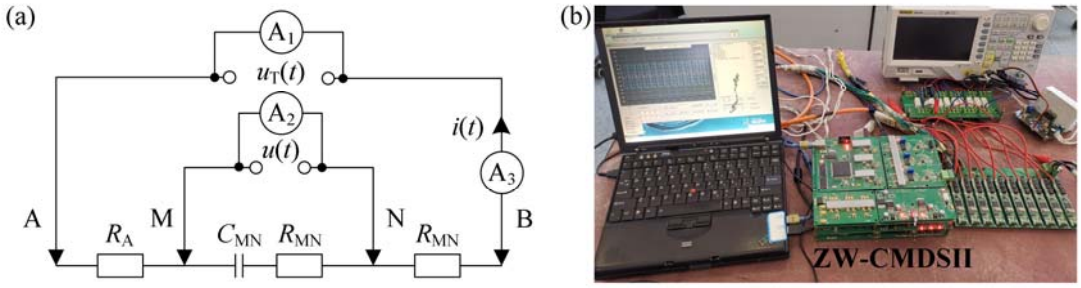

Figure 5. (a) Experimental schematic; (b) Experimental setup.

c. You try to sell the algorithm for handling IP data, so you need to show a section with the phase results. This was also pointed out by a previous reviewer. If you IP results are not satisfying due to low chargeability (as you write in your answer), then I suggest that you find another example. As a minimum, this should be included in a discussion.

Response.

Yes, we replace the simulation experiment with the resistance-capacitance experiment, present the recorded data and the forward response， and analyze the noise reduction performance on the frequency-spectrum (amplitude and phase) by the three algorithms.

Page 5 to 8

This modifications are as follows:

To validate the effectiveness of the ECI system, we performed a resistance-capacitance experiment, as shown in Figure 5.

The circuit parameters are chosen to be $R_{\mathrm{A}}=30.3\Omega/5\mathrm{W}$, $R_{\mathrm{MN}}=30.1\Omega/5\mathrm{W}$ $R_{\mathrm{B}}=30\Omega/5\mathrm{W}$ and $C_{\mathrm{MN}}=470\mu\mathrm{F}$. We recorded the applied voltage $u_{\mathrm{T}}(t)$, the injected current $i(t)$ and the measured potential signal $u(t)$ as the raw signals. These signals are a 3-order spread spectrum pseudo-random sequence at the clock cycle of 0.0125s, as shown in Figures 6a-c and Table 1.

Since our experiment is in a stable environment, we consider the system linear time-invariant and the noise from the current and voltage measurement are linearly superpositioned (Pelton, et al., 1983; De, et al., 1983; Vinegar and Waxman, 1984; De, et al., 1992; Garrouch and Sharma, 1998). Therefore, it is actually equivalent whether the noise is added to the injected current $i(t)$, the measured potential signal $u(t)$ or the applied voltage $u_{\mathrm{T}}(t)$. Therefore, the injected current $i(t)$ is only polluted by the synthetic background noise, including Gaussian and impulsive, as shown in Figures 6d and e. Thirdly, the complex resistivity of the main frequency is considered and discussed because the main energy of the pseudo-random signal is concentrated on the main frequency (He, 2017). Finally, for detailed comparisons between the ECI algorithm and the others, we add the synthetic Gaussian and impulsive noises to the response signal $i(t)$, respectively.

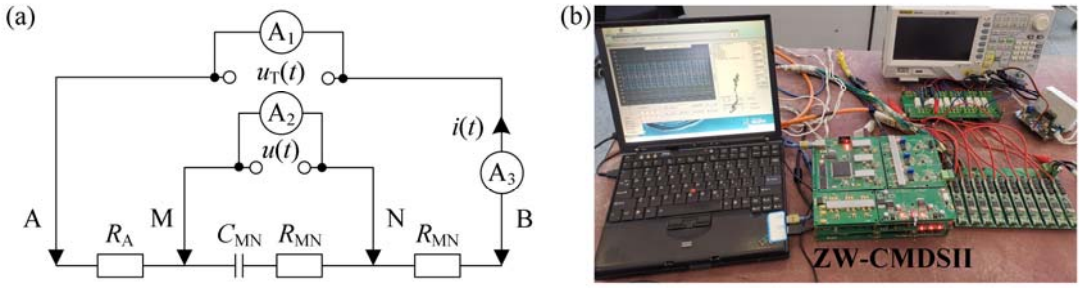

Figure 5. (a) Experimental schematic; (b) Experimental setup.

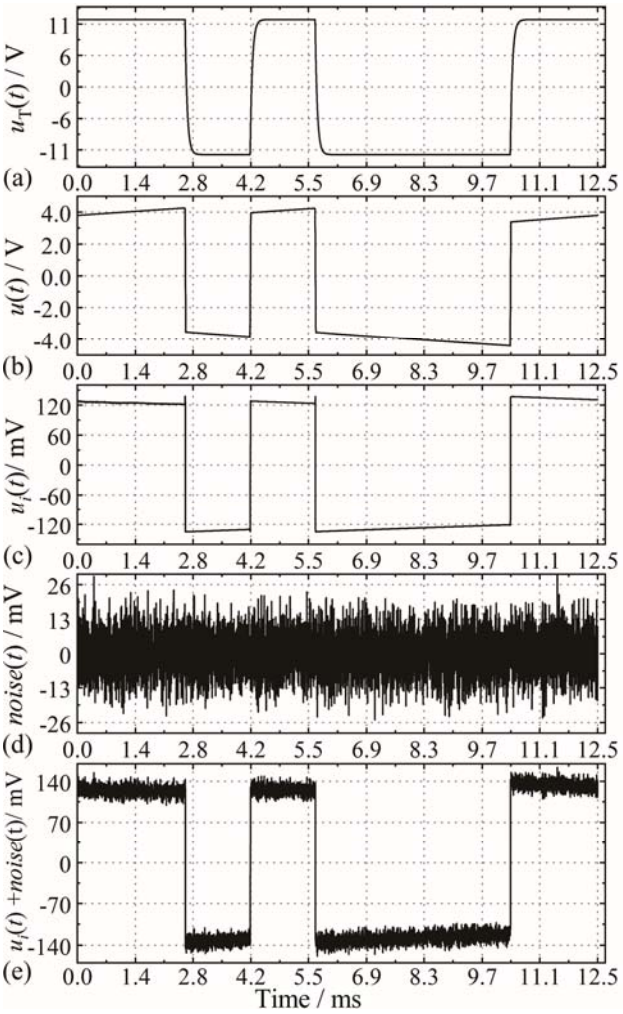

Figure 6. The time waves of (a) the applied voltage $u_T(t)$, (b) the measured potential signal u(t), (c) the voltage $u_i(t)$ at the sampling resistor

Table 1. Amplitude and phase values of complex resistivity obtained with Figures 6a-c.

Ftequency (Hz)	Theoretical amplitude (Ω)	Theoretical phase (rad)	Measured amplitude (Ω)	Measured phase (rad)
80.2	30.8	-0.14	30.8	-0.14
160.4	30.4	-0.07	30.3	-0.08
320.8	30.2	-0.03	30.7	-0.03

We use synthetic Gaussian noise with the deviation and mean values of 0.1 and 1.1 as a standard template. The excitation signal $i(t)$ is polluted by synthetic different energy levels of the Gaussian noise. Figure 7 show that the denoised results are obtained and compared at the three main frequencies when

the noise RMS ranges from 0.12 to 0.25. The figure shows that as the RMS of noise increases, the complex resistivity information obtained by each algorithm decreases. However, the amplitude spectrum after ECI processing has the slowest falling speed, and the phase spectrum has the slowest falling speed at 80 Hz.

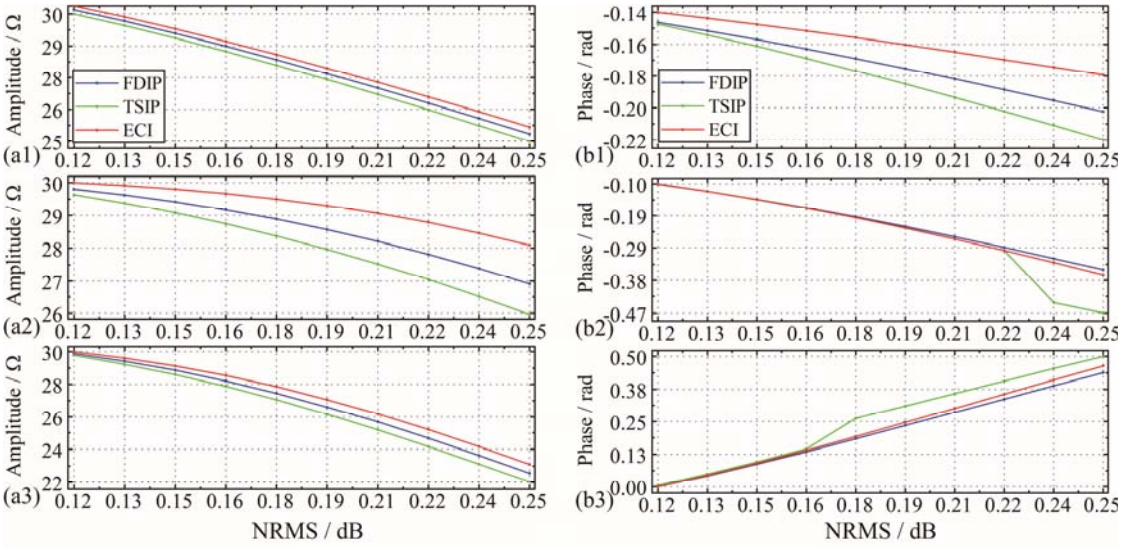

Figure 7. amplitude and phase of complex resistivity values at (a1) and (a2) 80 Hz, (b1) and (b2) 160 Hz, (c1) and (c2) 320 Hz comparison using the three methods.

Previous literature has shown that if the percentages of outliers in impulsive noise exceed 50%, the traditional denoising algorithm will be limited (Liu et al., 2016, 2017). Thus, Synthetic impulsive noise is added to the excitation signal $i(t)$ in ten percent steps. Their standard deviations (SDs) and skewnesses (SKs) are shown in Figure 8. As depicted in Figures 9, the three algorithms have a certain degree of denoising performance versus the different percentages of the synthetic outliers against the raw data. The figure shows that with the discrete points of impulse noise growing, the RMS of noise is different. The amplitude spectrum and phase spectrum of complex resistivity obtained by each algorithm fluctuate. Although the noise reduction performance of the phase spectrum processed by ECI does not stand out, the overall change of the amplitude spectrum after ECI processing is still slow, especially when the discrete point is more than 50%.

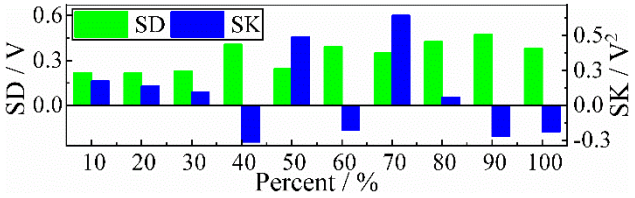

Figure 8. The standard deviations (SDs) and skewnesses (SKs) of synthetic impulsive noise.

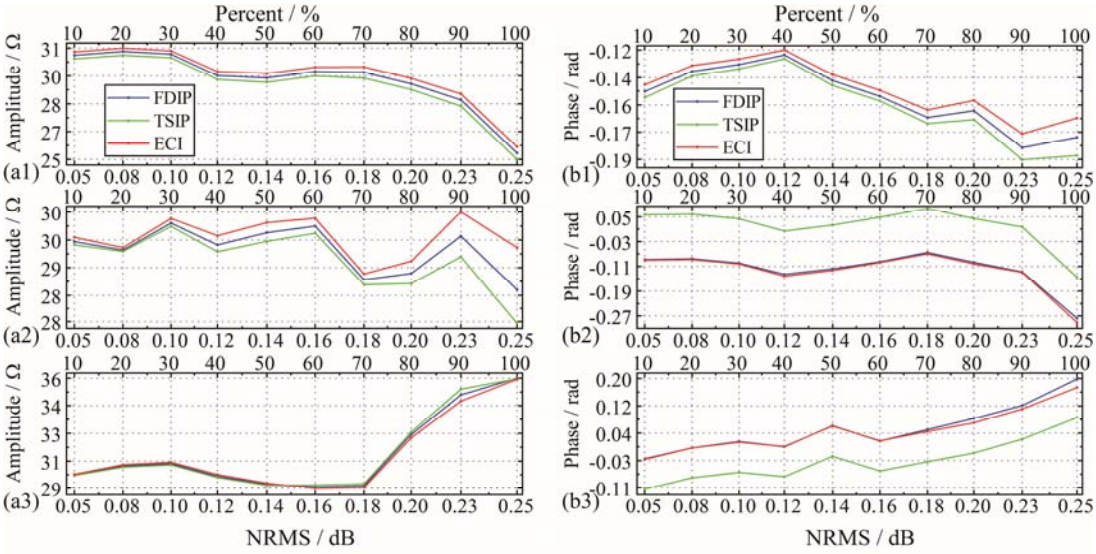

Figure 9. Complex resistivity values at (a1) and (a2) 80 Hz, (b1) and (b2) 160 Hz, (c1) and (c2) 320 Hz comparison using the three methods.

Comment 10. A discussion should be added in the manuscript with the answer to comment 5 from reviewer 1 (version 3).

Response.

Yes, we have added this discussion to the paper.

Page 4, Line 13 to 16.

This modifications is as follows:

Figure 4 shows the Schematic diagram of ZW-CMDSII (Zhang et al., 2014; He et al., 2014;). As is known from the figure, we are able to conclude that $u_T(t)$ is mainly disturbed by the floor noise energy of the instrument, and $i(t)$ and $u(t)$ are mainly contaminated by environmental noise. The floor noise is relatively very low, while environment noise possesses a much higher energy level. Thus we assume that $n_1(t) \approx 0$, and can conclude that zero correlation between $n_1(t)$ and $n_2(t)$, $n_3(t)$, $R_{n_1 n_2}(\tau) \approx 0$ and $R_{n_1 n_3}(\tau) \approx 0$.

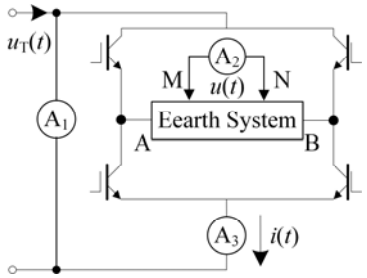

Figure 4. Schematic diagram of the instrument.

Comment 11. Is the code available for other researchers to use? Please add a section with code availability after the conclusion.

Response.

Sorry that we cannot open the code for public due to the confidentiality agreements of the funding.

However, we can provide the algorithm code for interested researchers via email (hsmfly1982@163.com).

Note:

We also add an expression in Eq. 13 ($=\left|\frac{P_{y_1y_2}(\omega)}{P_{y_1y_3}(\omega)}\right| e^{-j(\varphi_{y_1y_2}(\omega)-\varphi_{y_1y_3}(\omega))}$) to better illustrate the relationship between the amplitude and phase. This does not change any experiment results but we believe it could make the equations easier to understand.

Page 5, Line 5 and 6